Ionic bonding of transition-metal halides: A spectroscopic approach

J. Thomas
Laboratoire de Spectroscopie, Université de Rennes I, F-35042 Rennes, France
and Laboratoire d'Utilisation du Rayonnement Electromagnétique, Université de Paris—Sud, F-91045 Orsay, France

I. Pollini
Dipartimento di Fisica, Università degli Studi di Milano, via Celoria 16, I-20133 Milano, Italy;
Gruppo Nazionale di Struttura della Materia del Consiglio Nazionale delle Ricerche, I-20133 Milano, Italy;
and Laboratoire d'Utilisation du Rayonnement Electromagnétique, Université de Paris—Sud, F-91045 Orsay, France
(Received 23 July 1984; revised manuscript received 2 April 1985)

The dielectric theory of the chemical bond has been applied to crystals with either $Cd(OH)_2$ or $CdCl_2$ structure, namely to layered Mn, Fe, Co, and Ni dihalides (MX_2) with octahedral coordination, in order to evaluate the fractional ionic character f_i for this class of insulators. The crystalline spectroscopic energy gap E_g has been measured via the optical data, related to the dominant exciton peaks Γ, and then evaluated either through the Phillips model (E_g^{Phillips}) or the measured dielectric constant $\epsilon_1(0)$ in the framework of the Penn model (E_g^{Penn}). The obtained scales of ionicities, f_i or f_i^{DT}, ranging from $f_i \simeq 0.72$ of NiI_2 to $f_i \simeq 0.80$ of $MnCl_2$ are then compared to the ionicity scale f_i^{XPS} based on x-ray photoelectron spectroscopy. For transition-metal chlorides, for which photoemission spectra are available, the different ionicity scales are in good agreement. Furthermore, the ionicity parameters scale rather well with the ionicity trend given by the fitted values of the net charge Z, the electrostatic parameter for dealing with crystals not completely ionic. The overall agreement between the spectroscopically determined ionicity, the structural, thermochemical, and electronic properties of these compounds seems to indicate that the dielectric theory of Phillips and Van Vechten can be successfully applied to layered materials with reduced ionicity and open d-shell configuration.

I. INTRODUCTION

A quantitative measure of the ionicity of a chemical bonding is a useful concept to unify a number of experimental data. The balance between ionic and covalent bonding determines a number of structural, mechanical, vibrational, and electronic properties of semiconductors and insulators. For instance, the fundamental gap E_g increases in general with ionicity, while the dielectric constant $\epsilon_1(0)$ decreases; the splitting between longitudinal-optical (LO) and transverse-optical (TO) phonons at the zone center increases when the bond polarity is increased. A detailed discussion of the relation between these and other properties with ionicity is given by Phillips.[1,2] It is well known, however, that defining the ionicity of a chemical bond is not an easy task, although the concept of ionicity is very intuitive. Several attempts have been made to place this concept on firm ground either empirically or through one-electron quantum theory in terms of atomic orbitals.[3] Pauling resolved this problem by using the concept of resonating bonds.[4] The ionicity scale of Pauling, which is one of the oldest and still most widely used, is based on the observation that the heat of formation $H_f(AB)$ for a compound AB exceeds the average heat of formation $H_f(A)+H_f(B)/2$ of the elements A and B. This extraionic heat of formation $-\Delta H_f(AB)$ can be related to the electronegativities X_A and X_B and the number of resonating bonds per atom pair. Empirical estimates of $-\Delta H_f$ show that for a large number of bonds this extraionic heat of formation can be represented by

$$-\Delta H_f \sim (X_A - X_B)^2 .$$

The difference in the electronegativities determines the departure of the bond from the covalent limit and hence the ionic component of the bond.

Other ionicity scales express the ability of atoms to attract electrons through the mean value of electron affinity and ionization potentials.[5] Coulson's approach[6] defines the ionicity through the probability to find a valence electron on either of the two atoms A and B using trial wave functions based on atomic orbitals, and Harrison's method[7,8] relates the covalent and ionic contributions to the bonding in $A^N B^{8-N}$ compounds to matrix elements in an LCAO description of the valence bands.

The approach of Phillips and Van Vechten[9–12] (PVV) is based upon the spectral definition of ionicity, by reexamining the concepts of electronegativity in light of the quantum theory of the dielectric properties of crystals. The Phillips—Van Vechten scale has been also modified to be applicable to other than $A^N B^{8-N}$ compounds.[13,14] Another ionicity scale, which is similar to the Phillips—Van Vechten scale, and works well in practice, is derived from the photoemission spectra of the valence bands of compound semiconductors and insulators by exploiting the splitting of the low-lying s-like peaks in the density of states.[15,16]

The starting point of our investigations was the experi-

mental study of the high-frequency dielectric function $\epsilon(E)=\epsilon_1(E)+i\epsilon_2(E)$ of MX_2 (M=Fe, Co, Ni; X=Cl, Br, I) halides[17] in order to get the spectroscopic basis for determining the fractional ionic character (f_i) of the chemical bonds in transition-metal halides (TMH). The approach of the present paper[18] is to apply the theory, which has proven successful in the interpretation of the dielectric properties of semiconductors and alkali halides (NaCl type), to transition-metal halides [$Cd(OH)_2$ and $CdCl_2$ type]. MX_2 halides occur as strongly bonded two-dimensional X-M-X layers with weak interlayer coupling. Within a X-M-X sandwich, each metal atom is surrounded by six nearest-neighbor halogen atoms. The coordination of the halogen ions around the metal atom is octahedral.[19] The electronic structure of these materials can be presented schematically in the following way: the valence band, mainly constituted by the np levels (full) of the halogen (n=3,4,5), is separated by a "gap" from the conduction band formed from the empty levels $4s$, $4p$, . . . of the metal. The localized, partly filled, $3d^n$ levels of the metal (n=5,6,7,8) lie in this "gap." Such a configuration must produce several kinds of transitions: crystal field, charge transfer, orbital promotion, exciton, band-to-band transitions, according to the energy of excitation.

In Sec. II we first apply the PVV theory to the TMH by calculating the average Phillips gap (ionic and covalent parts) E_g^{Phillips} between filled (valence band) and unfilled (conduction band) states, and the related ionicity f_i. We show that E_g^{Phillips} is in good agreement with the optical gap E_g^{expt} obtained from reflectance spectra, and also that the octahedral coordination expected from the PVV theory (f_i value) is in agreement with the crystallographic structures of these compounds. Furthermore, we find that the ionicity f_i is well correlated to the value of the net charge Z, obtained through the fitting of thermochemical data and optical vibrational frequencies via a phenomenological potential.[20] Then, we calculate the Penn gap E_g^{Penn}, starting from the experimental value of the optical dielectric constant $\epsilon_1(0)$, in order to take into account the influence of the localized and partially filled $3d$ levels. We can thus evaluate, by means of the E_g^{Penn} value and the homopolar (heteropolar) part of the PVV theory, another value of the ionicity f_i^{DT} ($f_i'^{\text{DT}}$) which can be compared to f_i.

In Sec. III we compare the list of ionicities f_i, f_i^{DT} (or $f_i'^{\text{DT}}$) with the values obtained from the XPS scale, based on x-ray photoemission spectra of the valence bands (f_i^{XPS}). Finally, in Sec. IV the transferability of the PVV theory to the TMH is briefly discussed and the conclusions are presented.

II. IONICITY AND STRUCTURE ACCORDING TO THE PVV THEORY

Several models have been proposed to describe the dielectric properties of semiconductors and insulators, and a general theory of the dielectric response of a crystal to an external electric field of wave vector $\mathbf{q}$ and frequency ω in terms of a complex, nonlocal dielectric tensor $\underline{\epsilon}_1(\mathbf{q},\omega)+i\underline{\epsilon}_2(\mathbf{q},\omega)$ has also been formulated.[21] In the dielectric theory (DT) the lattice is regarded as a framework of positively charged ions screened somehow by valence electrons. For tetrahedrally coordinated semiconductors[9,10] (diamond, zinc-blende, and wurtzite crystals) and octahedrally coordinated NaCl-type insulators[11,12] (alkali halides), Phillips and Van Vechten suggested that such a model may be used in order to define the ionicity of a chemical bonding. They defined the average separation E_g^{Phillips} (Phillips gap) of the valence and conduction bands as the pythagorean sum of an ionic part C (Phillips electronegativity) and a covalent part E_h:

$$E_g^{\text{Phillips}}=(E_h^2+C^2)^{1/2} . \tag{1}$$

The homopolar energy gap E_h scales with the nearest-neighbor distance $d_{M\text{-}X}$ only like

$$E_h=ad_{M\text{-}X}^{-2.5}, \quad a\simeq 40.5 . \tag{2}$$

The ionic energy C can be defined through the Phillips electronegativity by

$$C(AB)=b\left[\frac{Z_A}{r_A}-\frac{Z_B}{r_B}\right]e^{-K_sR} , \tag{3}$$

with $R=r_A+r_B/2$ and $b\simeq 1.5$. The atomic radii r_A and r_B are defined as half of the bond length of the group-IV element belonging to the same row of the Periodic Table as atoms A and B, respectively. Z_A and Z_B are the valence numbers of elements A and B and K_s is the Thomas-Fermi screening parameter: $K_s=(4K_f/\pi a_0)^{1/2}$, where a_0 is the Bohr radius and K_f is the wave number on the surface of the Fermi sphere in the free-electron approximation. Phillips defines the fraction of ionic character of a chemical bond by

$$f_i=\frac{C^2}{(E_g^{\text{Phillips}})^2}=\frac{C^2}{E_h^2+C^2} . \tag{4}$$

We notice that a characteristic feature of the PVV theory is that the crystal structure does not appear explicitly anywhere, and therefore the model may be extended to include crystals belonging to the NaCl structure or is applicable to compounds other than A^NB^{8-N}.[13,14] Recently, the model has been also applied to structures of the CdI_2-type ($C6$), i.e., to SnS_2 and $SnSe_2$ crystals.[22] In the case of TMH, it is easily checked that the number of electrons involved in the chemical bonds is 16, eight per bond (neglecting the $3d$ electrons). We have then reported in Table I the crystallographic data of the MX_2 compounds, the Phillips gap, E_g^{Phillips}, the calculated values of C, E_h, the experimental gap E_g^{expt}, and the ionicity f_i.

The values of the Phillips gap E_g^{Phillips} have been calculated from Eqs. (1)–(3) with the values of the prefactor b (1.55±0.07) adjusted to reach a good agreement with the known experimental data.

Ultraviolet (uv) spectra[17,23,24] and soft-x-ray spectra[25] of MX_2 compounds are available in literature, and show prominent excitonic peaks close to the energy region, where the transitions from the outermost np orbitals of the halogen (n=3, 4, and 5 for Cl, Br, and I) to the $4s$ orbital of the transition metal occur. We consider as an appropriate value for the experimental energy gap E_g^{expt}, the average energy of the components of the exciton doublet

TABLE I. Crystal structures and lattice parameters. The Phillips ionicities f_i are calculated, together with the electronegativity C and the covalent gap E_h, from Eqs. (1) to (3). The value of the experimental gap E_g^{expt} is identified with the average energy of the prominent exciton peaks Γ_{ex}, and is compared to the Phillips gap E_g^{Phillips}.

Crystal	Type	a (Å)	$H:c$ $R:c/3$ (Å)	$d_{M\text{-}X}$ (Å)	$d_{X\text{-}X}$ (Å)	E_g^{expt} (eV)	E_g^{Phillips} (eV)	E_h (eV)	C (eV)	b	f_i
$MnCl_2$	R[a]	3.685	5.823	2.57	3.63	8.3[d]	8.38	3.79	7.47	1.59	0.795
$FeCl_2$	R[b]	3.603	5.845	2.55	3.59	8.3	8.28	3.86	7.33	1.59	0.783
$CoCl_2$	R[b]	3.553	5.786	2.52	3.55	8.3	8.28	3.98	7.26	1.60	0.769
$NiCl_2$	R[c]	3.478	5.801	2.49	3.51	8.4	8.31	4.10	7.22	1.62	0.756
$MnBr_2$	H[a]	3.82	6.19	2.69	3.81	7.7[d]	7.42	3.41	6.58	1.48	0.789
$FeBr_2$	H[b]	3.772	6.223	2.67	3.78	7.4	7.40	3.48	6.53	1.48	0.779
$CoBr_2$	H[b]	3.728	6.169	2.64	3.75	7.4	7.40	3.58	6.48	1.49	0.766
$NiBr_2$	R[a]	3.708	6.1	2.61	3.72	7.5	7.40	3.68	6.42	1.49	0.753
MnI_2	H[a]	4.16	6.82	2.94	4.17	5.2[e]	5.86	2.73	5.18	1.52	0.783
FeI_2	H[a]	4.04	6.75	2.87	4.08	6.0	5.97	2.90	5.21	1.58	0.764
CoI_2	H[a]	3.96	6.65	2.82	4.01	6.0	5.95	3.03	5.12	1.59	0.741
NiI_2	R[a]	3.89	6.54	2.77	3.94	6.0	6.00	3.16	5.10	1.62	0.722

[a]R. W. G. Wyckoff (Ref. 19).
[b]A. Ferrari *et al.*, Acta Crystallogr. **16**, 846 (1963).
[c]M. K. Wilkinson *et al.*, Phys. Rev. **113**, 497 (1959).
[d]Absorption peaks taken on annealed evaporated films (Sakisaka *et al.*, Ref. 26).
[e]M. R. Tubbs, Phys. Status Solidi **28**, K135 (1968).

Γ (Γ_{ex} in Fig. 1) rather than to the weak edge-like absorption steps, which in TMH (as in alkali halides) occur on the high-energy side of the first exciton peak Γ. This was preferred because it is sometimes difficult to estimate the values of E_g^{expt} in some compounds, as for instance in TM iodides, like FeI_2 and CoI_2. This excitonic transition, yielding the strongest structure of the interband edge in uv reflectance,[17,23] and absorption spectra,[24] occurs around 8.3 eV in transition-metal (TM) chlorides, 7.5 eV in TM bromides, and 6.0 eV in TM iodides.

We notice that these energy positions are mainly dependent on the nature of the anion and rather independent on that of the cation. On the other hand, the strongest charge transfer transitions occurring just before the excitonic transition shift according to the second ionization potential of the cation, thus denoting the $3d$ levels as final states. Thus, in order to calculate the forbidden energy gap between the halogen np levels and the metal $4s$ levels in the framework of the PVV theory, it seems reasonable to neglect the contribution of the localized partially filled $3d$ levels of metal in Eq. (3). As shown in Fig. 2, the Γ_{ex} exciton average energy E_g^{expt} can be related to the calculated values of Phillips energy gap E_g^{Phillips} with a very good agreement. We consider this correspondence between the experimental and calculated values and the fact that b is almost constant (and very close to the value $b=1.5$ employed by Phillips for $A^N B^{8-N}$ semiconductors) as necessary requisites for extending the calculation of ionicity to TMH.

For what concerns the ionicity, we notice that the trend

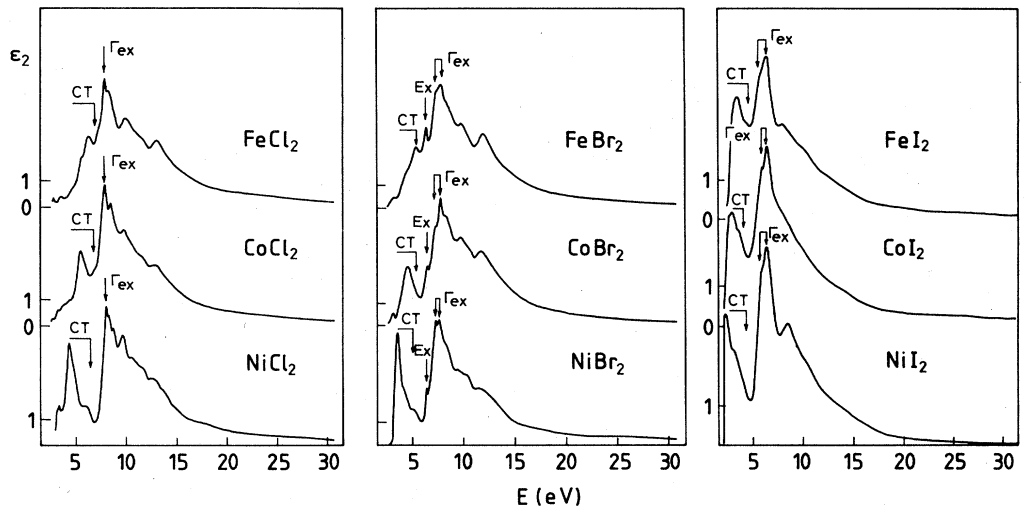

FIG. 1. Spectral dependence of the imaginary part, $\epsilon_2(E)$, of the dielectric function for Fe, Co, and Ni halides at room temperature (Refs. 17 and 23). The average value of the energy of Γ_{ex} excitons has been compared in the text with the calculated Phillips and Penn gaps. At lower energies charge transfer (CT) transitions ($p \rightarrow d$) show up.

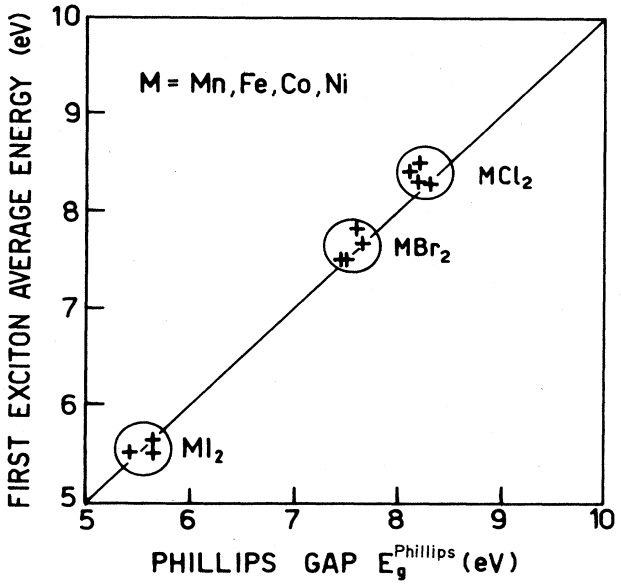

FIG. 2. Average peak energy of Γ_{ex} excitons observed in TMH versus the Phillips gap E_g^{Phillips}.

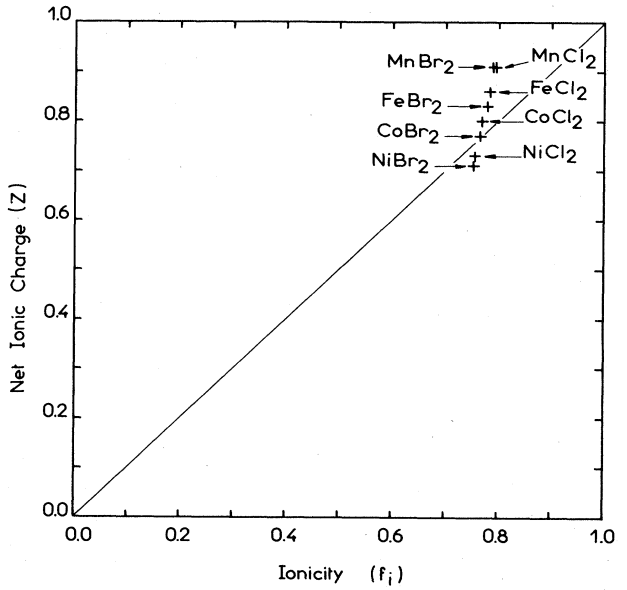

FIG. 3. Net ionic charge Z of crystal $3d$-metal dihalides (from Benedek and Frey, Ref. 20) versus the fraction of ionic character f_i of the dielectric theory of PVV.

of f_i, from $FeCl_2$ to NiI_2 (0.78 to 0.72) is, in general, consistent with the trend of $\epsilon_1(0)$ of TMH varying from 3.3 in $FeCl_2$ to about 4.4 in NiI_2. This agreement is expected from the DT, which predicts a decrease of the ionicity with increasing the dielectric constant. General chemiphysical considerations about the ionicity of halide compounds lead to the same result, i.e., usually the fluoride compounds are more ionic than the iodide's.

Benedek and Frey have defined the ionicity Z of TMH as the probability of finding an additional electron on the halogen atom and have calculated the value of Z by fitting the theoretical dispersion photon curves to the available neutron, Raman, and infrared data.[20] Now, if the crystals were composed of point-charge ions residing on the lattice sites (ideal ionic lattice) and if these charges were the only ones contributing to the effective Coulomb forces, then we would expect that f_i should be equal to Z. However, since there are both localized and nonlocalized contributions (as well as static and dynamic contributions to dynamical effective charges, which we do not consider in our discussion) to the value of Z and, besides, there is some uncertainty in the crystallographic and spectroscopic data of the real crystals, a certain amount of scatter must be expected. The values of the net ionic charge Z and those of the spectroscopic ionicity of the PVV, f_i, are both listed in Table II and graphically compared in Fig. 3. We can observe, anyhow, that for almost all the crystals the agreement is rather good.

In Table II we have also reported the values of U_0,[20] the cohesive energy of the ideal ionic lattice of TMH, which gives an estimate of the bond energy in the compounds and an indication of the ionicity of the bonding. Indeed, the heat of formation is connected with differences in the electronegativity of the elements; even more so, the greater the electronegativity difference between elements, the more ionic the bond and the greater the heat of formation. The values of U_0 have been obtained from the Born-Haber cycle[26,27] performed with the available thermodynamical data for TMH.[28] Since we are dealing with nearly ionic crystals the net halogen charge is $-eZ$, with $Z<1$. This implies that the expression of U_0 is affected by Z-dependent affinity energies and Z-dependent resonance energies, which represent the covalent contribution in a valence bond picture. A thorough discussion of the form $U_0(Z)$, given by Benedek and Frey,[20] shows what is lost, via the net charge reduction, by reducing the Madelung energy and what is gained in the formation of the partially covalent bond. For the cases in which Z has been calculated we see that $U_0(Z)$ is considerably lower than U_0, showing once again the fraction gained in the formation of the covalent bond in these partially ionic crystals. Thus, the lower the ionicity f_i, the greater the fraction of covalency $f_c=1-f_i$; in the same manner, the smaller Z is, the greater the ionic part lost in $U_0(Z)$ is. Of course we cannot push these considerations too far because the quantity $|U_0-U_0(Z)|$ is not connected in a simple way to the ionic and covalent parts f_i and f_c of the bond. However, if f_c is nearly equal to zero, we think that at least the trend of $|[U_0-U_0(Z)]/U_0|$ should roughly be the same of that of f_c [or the trend of $U_0(Z)/U_0$ the same of that of f_i]. In Fig. 4, where the ratio $U(Z)/U_0$ versus f_i has been plotted, one can see that a good agreement is found for the transition-metal chlorides and bromides.

One of the great successes of the DT is the correspondence between the ionicity and the coordination number for the $A^N B^{8-N}$ crystals. Phillips has found a critical value of f_i ($F_i=0.785$) which separates the fourfold coordinated from the sixfold coordinated structure, if the value of the ionicity f_i is lower or greater than 0.785, respectively. Kowalczyk *et al.*[15] have then extended these considerations to the case of $A^N B^{10-N}$ crystals, showing that the critical value of the Phillips scale should be

TABLE II. The experimental dielectric constants $\epsilon_{\text{eff},xx}^{\text{expt}} = \epsilon_{xx}(0)$ are calculated with Kramers-Kronig relation applied to ultraviolet reflectance data (Refs. 17 and 23) and are compared to the dielectric constants $\epsilon_{xx}^{\text{ESM}}(\infty)$ of the extended shell model (ESM). The values of the experimental (E_g^{expt}) and Penn (E_g^{Penn}) gaps are listed for comparison together with the two sets of DT and XPS ionicities. The ionic net charge Z and the cohesive energies for real and ideal ionic lattices are also reported (Ref. 20) in columns X, XII, and XIII.

Crystal	ϵ_{eff}	ϵ^{ESM}	$\hbar\omega_p$ (eV)	N_{eff}	E_g^{expt} (eV)	E_g^{Penn} (eV)	f_i^{DT}	f_i^{XPS}	Z^{d}	f_i	$U_0(Z)^{\text{e}}U_0$ (kcal/mole)	
$MnCl_2$					8.3			0.79[a]	0.91	0.795	505	605.1
$FeCl_2$	3.35	3.34	15.9	13.8	8.3	9.5	0.84	0.76	0.86	0.783	480	626.7
$CoCl_2$	3.50	3.31	16.2	13.1	8.3	9.4	0.82	0.75	0.80	0.769	431	645.0
$NiCl_2$	3.75	3.43	16.5	13.2	8.4	9.2	0.80	0.75[b]	0.73	0.756	402	663.9
$MnBr_2$					7.7			0.79[c]	0.91	0.789	479	587.9
$FeBr_2$	3.94	3.83	14.7	16.8	7.4	7.9	0.81	0.79	0.83	0.779	438	612.6
$CoBr_2$	3.89	3.91	14.9	16.4	7.4	8.1	0.81	0.79	0.77	0.766	401	630.0
$NiBr_2$	3.98	3.92	15.1	14.3	7.5	8.1	0.79	0.79	0.71	0.753	378	650.0
MnI_2					5.2			0.80[c]		0.783		567.9
FeI_2	3.82		13.2	12.2	6.0	7.2	0.84	0.80		0.764		593.9
CoI_2	4.00		13.6	12.8	6.0	7.2	0.82	0.80		0.741		610.3
NiI_2	4.36		13.9	13.5	6.0	7.0	0.80	0.80		0.722		627.7

[a]From photoemission data of Y. Sakisaka *et al.* (Ref. 24).
[b]From XPS data of Hufner and Wertheim (Ref. 36).
[c]Estimated average values for TM bromides and iodides from Refs. 16 and 39. All values are indicative.
[d]From Ref. 20. Also compare the values of $\epsilon_{xx}^{(\infty)} = 3.7$ and $Z = 0.75$ of VI_2 with the values of f_i (Table I) calculated for TMI.
[e]G. Benedek (private communication); and I. Pollini and G. Spinolo (unpublished data).

lowered to 0.71 in order to achieve a better accuracy when including other types of crystals than those of the $A^N B^{8-N}$ family. Thus, following Phillips, we have given in Cartesian plot the ionic contribution C versus the homopolar energy E_h (Fig. 5). We have found that some of the crystals are located near or above the critical value F_i fulfilling the predictions about their crystal structure, while other ones have values of f_i between 0.71 and 0.785. Thus, it seems reasonable also in this case to lower the critical value to $F_i = 0.71$, as suggested by Kowalczyk *et al.*, in order to take into account all the structures of the family of TMH.

One may notice, at this point, that there is quite a general agreement between the parameters calculated within the framework of the PVV theory (E_g^{Phillips}, f_i) and the spectroscopic values (E_g^{expt}), the thermochemical and structural data (coordination number) or the net charge Z obtained through dynamical considerations. Thus, it seems safe to conclude that, in a first approximation, the PVV theory can be successfully applied to layered

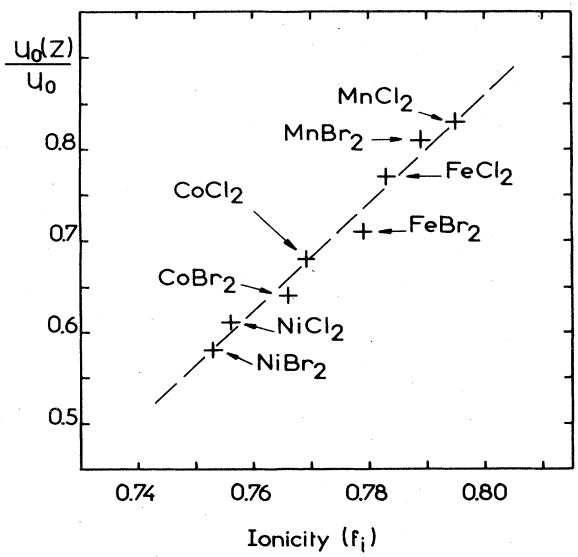

FIG. 4. Plot of the relative cohesive energy $U_0(Z)/U_0$ versus f_i for the TMH family.

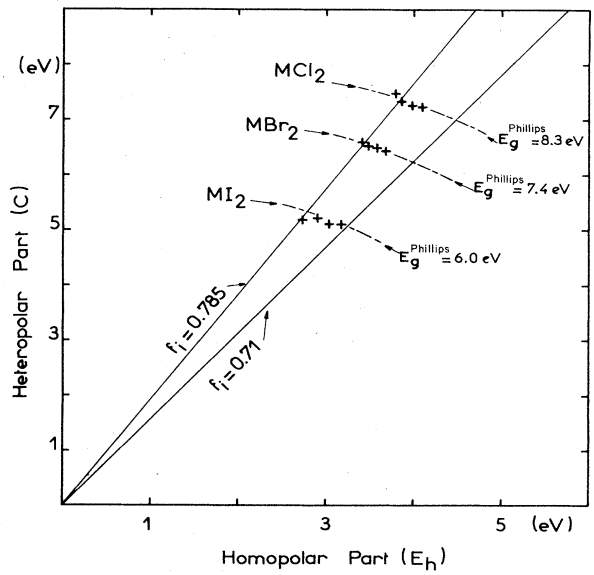

FIG. 5. TMH structures placed on an (E_h, C) average energy gap plot. Here E_h and C have been determined from Eqs. (2) and (3) and from the bond length $d_{M\text{-}X}$. The line $F_i = 0.785$ separates covalent structures with fourfold coordination from ionic structures with sixfold coordination. The critical ionicity $F_i = 0.71$ proposed by Kowalczyk *et al.* (Ref. 15) also permits prediction of the structures of binary $A^N B^{10-N}$ crystals.

transition-metal dihalides without taking into account the effect of the d shell, whose contribution will be considered below.

Since the presence of the open $3d$ shell may affect the measured values of the effective dielectric constant $\epsilon_{\text{eff}}(E)$ and effective number of valence electrons participating in the optical transitions, it is necessary to check the order of magnitude of this contribution to the ionicity by considering the Van Vechten modification[11] of the Phillips theory applied to the Penn model.[29]

In the framework of this model the average energy gap E_g^{Penn} (Penn gap) can be obtained from the low-frequency (low with respect to electronic frequencies, but high with respect to lattice frequencies) dielectric constant $\epsilon_1(0)$. If there are no important contributions to $\epsilon_1(0)$ from the d-shell polarization, Phillips relates $\epsilon_1(0)$ to the Penn gap E_g^{Penn} by the equation

$$\epsilon_1(0)=1+\left[\frac{\hbar\omega_p}{E_g^{\text{Penn}}}\right]^2\left|1-\frac{E_g^{\text{Penn}}}{4E_F}+\frac{1}{3}\left[\frac{E_g^{\text{Penn}}}{4E_F}\right]^2\right|^{1/2}, \tag{5}$$

where E_F is the Fermi energy in the free-electron model and ω_p is the plasma frequency:

$$\omega_p=\left[\frac{4\pi e^2 N}{m}\right]^{1/2}$$

with N electrons per atomic (or molecular) volume which contribute to the dielectric response. We may notice that the form of Eq. (5) is common in the elementary discussion of the optical properties of semiconductors.[30] When d-shell effects seem more important, we can include a modified version[11] of Eq. (5) in our program, obtaining thus the following expression for the Penn gap:

$$\epsilon_1(0)=1+\left[\frac{\hbar\omega_p}{E_g^{\text{Penn}}}\right]^2\left[\frac{N_{\text{eff}}}{N}\right]^{1/2}\times\left|1-\frac{E_g^{\text{Penn}}}{4E_F}+\tfrac{1}{3}(E_g^{\text{Penn}}/4E_F)^2\right|^{1/2}. \tag{5'}$$

The contribution of the d shell is reflected by a rise in $N_{\text{eff}}(E)$ and also in the saturation value of $\epsilon_{\text{eff}}^{\text{sat}}(E)\simeq\epsilon_1(0)$. The Kramers-Krönig inversion relations and the usual sum rules for ϵ_{eff} and N_{eff} applied to optical spectra lead us to calculate the appropriate value of E_g^{Penn} by using Eqs. (5) or (5'). The Penn gap is to be regarded as a sum of ionic and covalent parts, just as in Eq. (1). Moreover, we assume that the covalent part E_h can be written as

$$E_h^2=E_h^2(\overline{\text{IV}})(d^{\overline{\text{IV}}}/d)^5,$$

where $d^{\overline{\text{IV}}}$ is the crystal lattice constant, d is the metal-halogen distance ($d_{M\text{-}X}$) in TMH, and $E_h(\overline{\text{IV}})$ is the gap energy for the homopolar crystals belonging to the fourth-row elements. This follows the Phillips scaling between the lattice constant d and E_h for the fourth-row compounds, as expressed in Eq. (2). These relations allow one to calculate the fraction of ionic character of the chemical bond by using the relation

$$f_i^{\text{DT}}=1-\left[\frac{E_h}{E_g^{\text{Penn}}}\right]^2, \tag{6}$$

which is very similar to Eq. (4) of the PVV theory. In our application of the Penn model we have at first neglected the effect of the d-shell electrons and taken $N=12$, that is 12 electrons per unit cell, when computing ω_p and N_{eff} (fourth and fifth columns of Table II). In this case, one can correct Eq. (5) in this effect by considering a factor $N_{\text{eff}}(E)/N\geq 1$ in Eq. (5'). If we consider $N_{\text{eff}}\neq 12$ and recalculate the Penn gap E_g^{Penn} and the ionicity f_i^{DT} we find a general increase of f_i^{DT} and E_g^{Penn} along the crystal series, as is evident from the form of Eq. (5). It is nevertheless interesting to report the average values of f_i^{DT} and E_g for the families of chlorides, bromides, and iodides in Table III in order to indicate the true magnitude of Van Vechten's correction and to illustrate its possible influence on the "absolute values" of the ionicity. Thus, passing from chlorides to iodides, we have found that for MCl_2: $0.81\leq f_i^{\text{DT}}\leq 0.83$; for MBr_2: $0.8\leq f_i^{\text{DT}}\leq 0.84$; for MI_2: $0.82\leq f_i^{\text{DT}}\leq 0.83$; and for the Penn gap: $9.4<E_g^{\text{Penn}}<9.8$ eV, $8.0<E_g^{\text{Penn}}<9.1$ eV, and $7.1<E_g^{\text{Penn}}<7.3$ eV. We see that the ionicity values and the Penn gap energies do not change much when $N_{\text{eff}}\neq 12$, but it seems that VV modification leads to a slight overevaluation both for the ionicity and the energy-gap parameters. Table II presents the E_g^{Penn} and f_i^{DT} values obtained in this way together with the values of Z and $\epsilon_{xx}^{\text{ESM}}$ obtained from the extended-shell-model (ESM) calculation.

The ionicities f_i and f_i^{DT} of the PVV theory give practically the same results for TM chlorides and TM bromides as it appears from a perusal of columns XI and VIII of Table II, although the trend of ionicities presented by f_i (Table I) seems more in keeping with the general chemical knowledge. Instead, the values of f_i^{DT} concerning TMI look somewhat higher than expected on the ground, for instance, of the values of the measured and calculated dielectric constant (columns II and III of Table II) or the magnitude of the experimental gap E_g^{expt}. This is a little more striking also in consideration of the fact that the behavior of f_i shows no sign of anomaly along the ionicity scale from TMC to TMI. We are inclined to think that the ionicity overevaluation given by the parameter f_i^{DT} to TMI can be ascribed to a kind of "size effect" working when one evaluate the homopolar gap E_h, which is only function of the M-X distance according to Eq. (2). In this way, ions presenting the same value of $d_{M\text{-}X}$ and great differences in ionic radii would give the same covalent contribution to the bond, contrarily to physical intuition. Now, this systematic error has its greatest effect in the case of TMI, where E_h is underestimated without any compensation. Instead, when one determines the Phillips gap through Eqs. (1)—(3), one can partially compensate for this error the final result (E_g^{Phillips}) by calculating the Phillips electronegativity C, where the ionic radii are taken into account.

Starting from the Penn gap one can also evaluate the ionicity by Eq. (7): $f'^{\text{DT}}=(C/E_g^{\text{Penn}})^2$, where the ionic part C is calculated by means of Eq. (3), with the same value of the prefactor b ($\simeq 1.55$). This leads to an aver-

TABLE III. Average values of the Penn gap $\overline{E}_g^{\text{Penn}}$ and the ionicity $\overline{f}_1^{\text{DT}}$ for the chloride, bromide, and iodide families, in the framework of the Penn model. The effects of the d-shell electrons are taken into account by considering the Van Vechten modification of the Phillips model. These average values are then compared to the average values of the experimental (excitonic) gap $\overline{E}_g^{\text{expt}}$, the Phillips gap, $\overline{E}_g^{\text{Phillips}}$, and the Phillips and XPS ionicities, $\overline{f}_i$ and $\overline{f}_i^{\text{XPS}}$. ($M$: Mn, Fe, Co, Ni.)

	$N_{\text{eff}}/N=1$		$N_{\text{eff}}/N\neq 1$					
Crystal	$\overline{E}_g^{\text{Penn}}$ (eV)	$\overline{f}_i^{\text{DT}}$	$\overline{E}_g^{\text{Penn}}$ (eV)	$\overline{f}_i^{\text{DT}}$	$\overline{E}_g^{\text{expt}}$ (eV)	$\overline{E}_g^{\text{Phillips}}$ (eV)	$\overline{f}_i$	$\overline{f}_i^{\text{XPS}}$
MCl_2	9.4	0.81	9.8	0.83	8.3	8.3	0.78	0.78
MBr_2	8.0	0.80	9.1	0.84	7.5	7.4	0.77	0.79
MI_2	7.1	0.82	7.3	0.83	5.8	6.0	0.75	0.80

age value of $f_i'^{\text{DT}}$ equal to 0.60, 0.70, and 0.50 for the chlorides, the bromides, and the iodides, respectively. As one can see, the chemical trend is not respected in this case: the ionicity value for the bromides is higher than the ionicity for chlorides by more than 10%. Moreover, the homopolar part $E_h=[(E_g^{\text{Penn}})^2-C^2]^{1/2}$ does not scale with Eq. (2), where the constant $a=40.5$. If we would try to correct these anomalies in order to get the correct order of magnitude either of the Phillips ionicity f_i, or the XPS ionicity, f_i^{XPS}, one should take for the prefactor b of Eq. (3) values of 1.8 and 1.65 for the chlorides and the bromides, respectively, and parallel, the constant a of Eq. (2) would vary from 42 to a value of 44. We cannot, however, proceed much further with these arguments, since the discrepancies which have been found are mainly originated by the form of the Phillips electronegativity [see Eq. (3)], where one cannot see how to consider the values of Z_B and r_B, when the d electrons of the cations are taken into account in the calculation of the ionicity.

In conclusion, we notice that in order to take into account the modification of the ionicity values of TMH induced by the presence of the $3d$ levels in the forbidden gap, the use of the Penn gap energy E_g^{Penn}, determined by means of Eq. (5) together with Eq. (6), gives values of the ionicities slightly overevaluated, but rather close to the values obtained by means of the PVV theory, except for those of iodides. On the other hand, when we consider the definition of f'^{DT} using the Penn gap and, as a second parameter, C, we find a slight variation of b in Eq. (3) and also that the Eq. (2) for E_h is not followed with $a=40.5$. In the two cases the discrepancies are not drastic: in effect, the order of magnitude of the ionicities f_i and f_i^{DT} (0.7–0.8) is respected, showing that one can practically disregard the influence of the $3d$ levels in the ionicity determination for these compounds. Furthermore these discrepancies are probably be due to the fact that E_g^{Penn} is not the most appropriate parameter, since we apply the isotropic Penn model to anisotropic compounds. Also, the ϵ_{eff} value has been obtained though the usual sum rule in which the imaginary part of the dielectric function is obtained from optical data with the electric field vector of the incident radiation perpendicular to c axis. In fact, ϵ_{eff} only gives the contribution of the ϵ_{xx} component of the $\hat{\epsilon}$ tensor, whose other terms $\epsilon_{yy}=\epsilon_{xx}$ and ϵ_{zz} are not considered.

III. DT AND XPS IONICITY SCALES

In search of a more direct determination of the ionicity parameter, let us now consider other available experimental information and discuss the ionicity scale based on valence-band spectra. It is in fact possible to define an ionicity f_i^{XPS} (x-ray photoelectron spectroscopy), which makes use of the splitting of the low-lying s-like peaks in the density of states of semiconductors.[15,16] By s-like, one means that the charge density is concerned on the atomic sites, while, by p-like, it is considered that the charge density is concentrated between the atomic sites in bonding regions. For example, let us consider Fig. 4 of Ref. 16 (or Fig. 1 of Ref. 15), where the separation ΔE_s of the XPS peaks (corresponding to bands 1 and 2 calculated by empirical pseudopotential methods[31–34]) increases in the isoelectronic series Ge, GaAs, ZnSe, and NaCl. We observe that the electronic charge densities calculated for several diamond and zinc-blende-type semiconductors[34] can be related to photoemission peaks in the spectra shown in Figs. 1 (Ref. 15) or 4 (Ref. 16). The low-energy peak (peak I) consists of electrons centered around the anion atomic site (s-like distribution) and the higher-energy peak (peak II) consists of electrons basically centered around the cation and located in the bonding region. The highest peak (peak III) results from electrons concentrated between the atomic sites in the bonding region (p-like distribution). We also remark that in alkali halides (and TMH) peaks II and III strongly overlap, giving only one peak in XPS spectra. It is also noticeable that, passing from Ge to ZnSe and alkali halides, the effect of increasing the antisymmetric part of the potential is to progressively unmix the s-p bands 1 and 2 (corresponding to experimental peaks I and II-III) into purer atomlike states. In this way ΔE_s can be related to the ionic character of the bonding. Since ΔE_s does not vanish for Ge (see Fig. 4 of Ref. 16), ΔE_s may be decomposed into its covalent (ΔE_s^c) and ionic (ΔE_s^i) contributions:

$$\Delta E_s=\Delta E_s^c+\Delta E_s^i\ , \tag{7}$$

and ΔE_s^c is identified with the splitting in the elemental semiconductor.[16] Furthermore, ΔE_s^c follows a simple linear relationship[35] as a function of the interatomic distance $d_{M\text{-}X}$,

$$\Delta E_s^c = 8.0 - 2.2 d_{M\text{-}X} \ , \tag{8}$$

with ΔE_s^c measured in eV and $d_{M\text{-}X}$ in Å. Thus also for heteropolar compounds MX_2, ΔE_s^c can be calculated according Eq. (8) and f_i^{XPS} is finally obtained from

$$f_i^{\mathrm{XPS}} = \frac{\Delta E_s^i}{\Delta E_s} \ , \tag{9}$$

with ΔE_s^i obtained as the difference between the experimentally observed splitting ΔE_s and the calculated covalent gap ΔE_s^c.

Let us now turn to TMH for which XPS (Refs. 24 and 36) and extreme ultraviolet photoemission[37,38] (EUPS) spectra are reported. We observe that the XPS spectra of $MnCl_2$, $FeCl_2$, $CoCl_2$, and $NiCl_2$ reported, together with the corresponding EUPS spectra, in Figs. 6 and 7 show

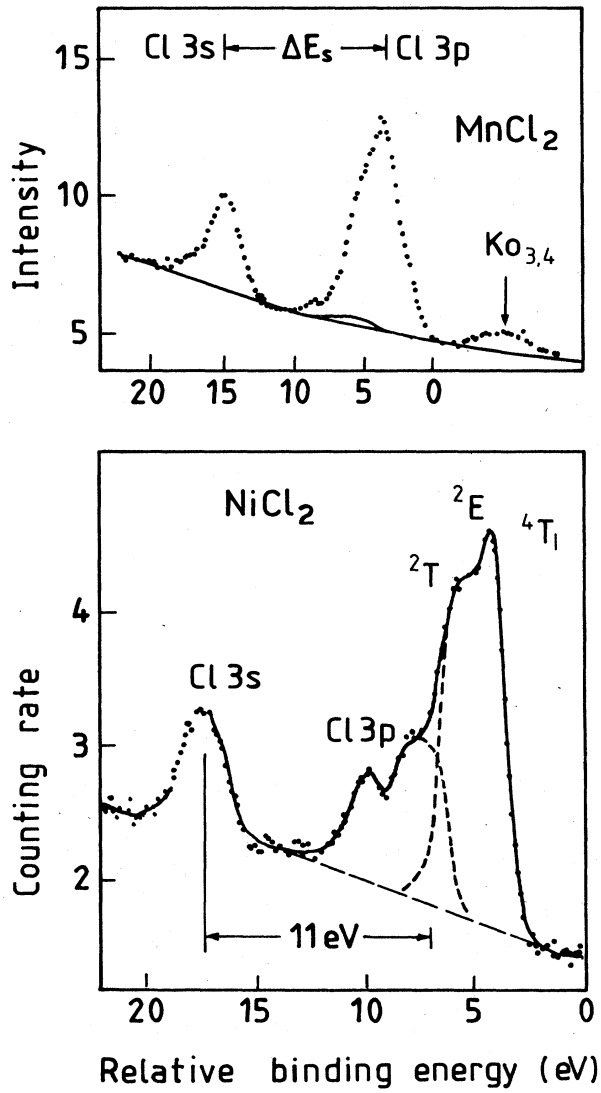

FIG. 6. XPS spectra of $MnCl_2$ (Sakisaka *et al.*, Ref. 24) and $NiCl_2$ (Hufner *et al.*, Ref. 36). The position of Cl 3*s* and 3*p* peaks are indicated, as well as the splitting ΔE_s. In the case of $NiCl_2$, the structure of the 3*d* band interpreted as the final-state structure in the $3d^7$ weak crystal-field notation is also shown.

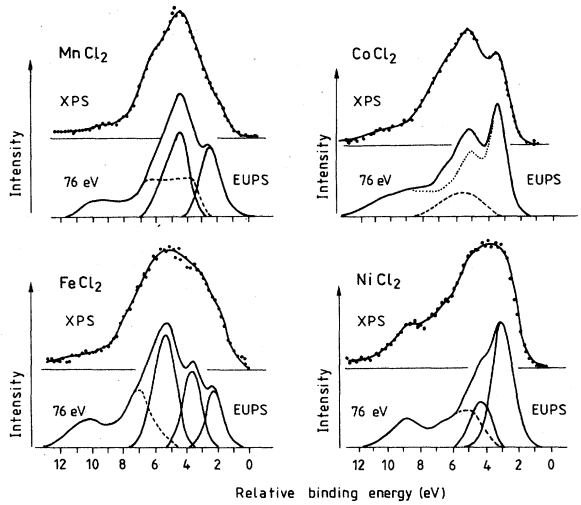

FIG. 7. Review of the valence-band XPS and EUPS photoemission spectra (Ishi *et al.*, Ref. 37), showing the component bands of the 3*d*-spectra in EUPS spectra for Mn, Fe, Co, and Ni chlorides. Dashed lines always indicate the contribution of the 3*p* states of chlorine.

that, far from being anomalous cases, the TMH demonstrate features in their valence-band densities of states similar to those found in the spectra of II-VI and III-V binary compounds,[15,16] and that these features evolve regularly in proceeding from the more covalent compounds to the ionic alkali and transition-metal halides. Thus, following the arguments developed by Kowalczyk *et al.*,[15,16] we shall try to calculate the XPS ionicity for the chloride series from an analysis of the XPS and EUPS spectra, reported from various sources[24,37,38] in Figs. 6 and 7. Let us first observe that the great energy separation between 3*s* and 3*p*-like levels in the XPS spectra of $MnCl_2$ (Ref. 24) and $NiCl_2$ (Ref. 36) and their overall resemblance suggest a bonding of predominant ionic nature in MX_2 materials as in alkali halides.[16] However, an important difference in the electronic structure of the uppermost valence band of TMH must be remarked in contrast with alkali halides. In fact, while in the latter compounds, the valence band is considered to be due to pure anion *p* levels, in TMH the valence state consist of a mixing of the cation 3*d* states with the 3*p* states of chlorine. Thus, the XPS spectra of MX_2 are strongly affected by the transition matrix elements between the metal 3*d* level or the halogen *np* level ($n=3,4$) and the nearly-free-electron state of excited electrons with large energy. In Fig. 7 the distribution of the 3*d* levels of Mn^{2+}, Fe^{2+}, Co^{2+}, and Ni^{2+} ions calculated by a ligand field treatment[37] is shown by lines under the EUPS spectra in order to have an indication of the cation *d*-state contributions and to estimate the valence-band top of the "pure" *p*-like states for TMH. This point is, of course, in relation with the evaluation of the value of ΔE_s and hence of f_i^{XPS}. The average separation between the 3*p*-like peaks and the 3*s*-like peak of chlorine is around 10—11 eV for all transition-metal (TM) chlorides.[24] We directly observe this energy separation between the XPS peaks of $MnCl_2$

and $NiCl_2$ crystals in Fig. 6. The same order of energy separation is found for the TM chlorides in the EUPS spectra between peaks B, originating from the Cl-3p states and the structure E, arising from the Cl-3s level (see Fig. 5 of Ref. 38). Indeed, the energy value of the peak E is near the binding energy of the 3s level of chlorine cited in the standard tables of the atomic energy levels.[39] Now, for heteropolar TM chlorides, ΔE_s^c is calculated according to Eq. (8) and the ionic gap ΔE_s^i is obtained as the difference between the observed splitting ΔE_s and ΔE_s^c. The procedure for obtaining f_i^{XPS} [see Eq. (9)] has given for TM chlorides the values reported in the ninth column of Table II. From the XPS spectra of the valence-band region of the sodium and potassium halides, shown in Figs. 2 and 3 of Ref. 16, we can have an estimate of the s-p splitting in alkali halides, which seems of the same order of magnitude of the halogen splitting reported in the standard table of x-ray energy levels.[39] In particular, the 3s-3p splitting (Cl) is about 10—11 eV, the 4s-4p (Br) splitting about 11—12 eV, and the 5s-5p (I) splitting around 10.5 eV. By considering the s-p splitting for TMH we could try to estimate the XPS ionicity for TM bromides and iodides (as an order of magnitude) whose average ionicity values we report in Table II. While for TM bromides the values of f_i^{XPS} reported in Table II still appear reasonable, the calculated values for TM iodides seem a little high (TMI are probably less ionic). We think that the overvalued figures of f_i^{XPS} of TMI are still due to the same kind of "size effect" which presents itself when we apply Eq. (8) to the iodine ions, thereby implying a systematic error in the evaluation of the homopolar contribution to the bonds.

We notice that the ionicity figures given by f_i^{DT} and f_i^{XPS} in Table II are very similar in both scales (leaving aside the case of TMI) and that the ionicity character of TM chlorides and bromides is almost the same. In conclusion, these compounds span a range of ionicities between 0.72 and 0.84 (see Tables I and II), which suggests a nonvanishing covalent contribution to the TMH's bonding. This signals a slight deviation from the pure ionic model of closed-shell ions interacting only through their electrostatic forces. The covalent contribution is in general reflected in the shape and width of the valence-band spectra, as it has been observed by different authors.[16,40] This analysis is also appropriate to the valence-band spectra of TMH measured by Sakisaka *et al.* (see Fig. 2 of Ref. 24). We can see, for instance, that for compounds with the same halogen, i.e., for the same atomic origin of the valence band, the anion-derived top peak in the XPS spectrum of the Ni halide (chloride or bromide) shows more structure than that of the corresponding Mn halide. In analogy to alkali halides,[16] this seems to indicate a higher degree of banding in Ni-halides than in Mn halides, in agreement with the lower ionicity of the former materials.

IV. CONCLUSIONS

A characteristic feature of the PVV theory is its applicability to different structures, ranging from the zinc-blende and wurzite-type crystals to NaCl structures. In fact, the DT has been used to extrapolate the dielectric properties of semiconductors to strongly ionic I-VIII crystals and also to $Cd(OH)_2$-type structures.[22] The ionicity scale we have employed for TMH assigns an ionicity f_i between 0 and 1 to each material so that the most covalent ones have small values of f_i (0.10—0.40) and the most ionic have f_i close to unity (0.75—0.95), e.g., the most ionic materials are alkali halides, such as RbF (0.96), KCl (0.953), KI (0.95), or NaBr (0.934) (see Table A of Ref. 12, for a list of 68 $A^N B^{8-N}$ compounds with f_i values predicted by Phillips, Pauling, and Coulson *et al.*[41]). The application of the PVV model to TMH has permitted the determination of the characteristic parameters as, for example, the Phillips gap E_g^{Phillips}, the ionicity f_i, and its relation to the expected coordination number of the crystal structures. These parameters have been compared to experimental data (i.e., E_g^{Phillips} has been correlated to E_g^{expt}, and f_i to f_i^{XPS}) or to calculated quantities (f_i has been typically correlated to the ionic net charge Z) in order to check the self-consistency of all these quantities. By considering the experimental errors, the involved approximations of the various models and the strong influence of the lattice parameters in the determination of the ionicity scales, we have found a good agreement between the spectroscopic ionicities based on the Phillips homopolar gap and electronegativity equations (f_i), the Penn gap found from $\epsilon_1(0)$ (f_i^{DT}) or determined from XPS and UPS spectra (f_i^{XPS}). When some discrepancy is found between the figures reported for f_i, f_i^{DT}, or f_i^{XPS}, as in the case of transition-metal iodides, where f_i^{DT} or f_i^{XPS} is always fairly larger than f_i, reasons for this fact have been put forward. A generalized version of the Phillips—Van Vechten scale has been then applied to MX_2 crystals in order to test the octahedral coordination of the transition-metal cations. Also, we have shown a close correlation between the spectroscopically determined ionicity and the net charge Z for dealing with crystals not completely ionic. The reported values of f_i calculated for MX_2 materials show that they are in general relatively ionic, passing from less ionic crystals like NiI_2 ($f_i \simeq 0.72$) to more ionic crystal like $MnCl_2$ ($f_i = 0.80$). The increasing values of the ionicity passing from NiX_2 to MnX_2 and the general lower ionicity of TM iodides are consistent with chemical expectations. The ionic character of MX_2 is also in agreement with the long bond length M-X close to the sum of ionic radii,[42] and the octahedral coordination of the cations, since this arrangement of the transition metals allows a greater anion-anion (X-X) separation with a corresponding reduction of the interionic repulsion.

Another general confirmation of the ionicity of TMH is the experimental finding, expected for relatively ionic materials, that they show the low-intensity many-electron d-state crystal-field spectra.[43—46]

The effect of the partly filled 3d shell has been neglected in a first application of the model since we have noticed from the optical spectra and $\epsilon_2(E)$ plots reported in Fig. 1 that the energy of the sharp, intense exciton peaks are not practically affected by the different electronic configurations of the $3d^n$ electrons through the series Mn to Ni halides ($3d^5$ to $3d^8$ configurations). Nevertheless, since the presence of the open 3d shell might affect the re-

sults of the usual sum rules on ϵ_{eff} and N_{eff}, we have also considered this contribution to the ionicity through the Van Vechten modification[11] of the Phillips theory. The results which have been shown in Table III are not very different from those obtained when the contribution of the $3d$ levels is neglected. This fact suggests that the $3d$ electrons are not valence electrons participating to the chemical bond, and also that the PVV theory can be applied to TMH disregarding the $3d$-shell contribution altogether.

Thus, we can conclude that the dielectric approach can prove fruitful not only for alkali halides but for TM salts as well[10,11] and the transferability of the PVV model should be valid notwithstanding the TMH, which have a full eight-electron s-p valence band per M-X band, also possess a narrow, localized $3d^n$ shell in the forbidden energy gap. The PVV model can also be employed to foresee the ionic character of other members of the TMH family on the basis of Eqs. (1)—(3) with the same values of the parameters a and b used for the layered TMH; for example, one could calculate the ionicity f_i for the series MF_2 (with M = Mn, Fe, Co, Ni) or extend the calculation of f_i to other first-row transition-metal compounds such as VX_2, CrX_2, or TiX_2 (X = F, Cl, Br, I), without any knowledge of the optical data. For these compounds, it would of course be useful to measure the optical spectra in a large energy range, if the data are lacking, in order to check the calculated quantities with the spectroscopic results, and correct, if necessary, any discrepancies by means of the useful experimental quantities, like $\epsilon_1(0)$ or E_g^{expt}, employed in the PVV model.

From the foregoing considerations, one can finally conclude that the PVV model constitutes a kind of general theory valid for many different types of crystals, ranging from the zinc-blende or wurtzite types to the rocksalt and $Cd(OH)_2$-$CdCl_2$ structures, where each crystal can be described either by the two parameters E_h and C or $\epsilon_1(0)$ and E_h.

ACKNOWLEDGMENTS

This work has been performed in the framework of the Scientific Cooperation Agreement between the Centre National de la Recherche Scientifique (France) and the Consiglio Nazionale delle Ricerche (Italy). Financial support under Grant No. 132.03.2/124138 has been given to one of us (I.P.) during his stay at the Université de Paris—Sud and the Université de Rennes I. The support of the staff of the Laboratoire de l'Accélération Linéaire (Orsay) de l'Université de Paris—Sud for providing the light beam during the experimental course is also greatly acknowledged by the authors.

[1] J. C. Phillips, *Covalent Bonding in Crystals, Molecules and Polymers* (The University of Chicago Press, Chicago, 1969).
[2] J. C. Philips, *Bond and Bands in Semiconductors* (Academic, New York, 1973).
[3] H. A. Skinner, Chem. Rev. **55**, 745 (1955).
[4] L. Pauling, *The Nature of Chemical Bond* (Cornell University Press, Ithaca, 1939).
[5] R. S. Mulliken, J. Chem. Phys. **2**, 782 (1934).
[6] C. A. Coulson, L. B. Redei, and D. Stocken, Proc. R. Soc. London **270**, 352 (1962).
[7] W. A. Harrison, Phys. Rev. B **10**, 767 (1974).
[8] W. A. Harrison and S. Ciraci, Phys. Rev. B **10**, 1516 (1974).
[9] J. C. Phillips, Phys. Rev. Lett. **20**, 550 (1968).
[10] J. C. Phillips and J. A. Van Vechten, Phys. Rev. Lett. **22**, 705 (1969).
[11] J. A. Van Vechten, Phys. Rev. **182**, 891 (1969).
[12] J. C. Phillips, Rev. Mod. Phys. **42**, 317 (1970), and references quoted therein.
[13] P. J. Stiles, Solid State Commun. **11**, 1063 (1972).
[14] D. Schiferl, Phys. Rev. B **10**, 3573 (1974).
[15] S. P. Kowalczyk, L. Ley, F. R. McFeely, and D. A. Shirley, J. Chem. Phys. **61**, 2850 (1974).
[16] S. P. Kowalczyk, F. R. McFeely, L. Ley, R. A. Pollak, and D. A. Shirley, Phys. Rev. B **9**, 3573 (1974).
[17] I. Pollini, G. Benedek, and J. Thomas, Phys. Rev. B **29**, 3617 (1984).
[18] This work was presented in the poster session at the *Fifth General Conference of the Condensed Matter Division of the European Physical Society, Berlin (Federal Republic of Germany)*, edited by D. H. Haberland and J. Treusch (European Physical Society, Geneva, 1985), Vol. 9A.
[19] R. W. G. Wyckoff, *Crystal Structures* (Wiley-Interscience, New York, 1963), Vol. I, p. 266.
[20] G. Benedek and A. Frey, Phys. Rev. B **21**, 2482 (1980).
[21] P. Nozières and D. Pines, Phys. Rev. **109**, 762 (1958); Nuovo Cimento **9**, 470 (1958).
[22] V. P. Gupta, P. Agarwal, A. Gupta, and V. K. Srivastava, J. Phys. Chem. Solids **43**, 291 (1982).
[23] I. Pollini, J. Thomas, and A. Lenselink, Phys. Rev. B **30**, 2140 (1984).
[24] Y. Sakisaka, T. Ishii, and T. Sagawa, J. Phys. Soc. Jpn. **36**, 1365 (1974); **36**, 1372 (1974).
[25] S. Sato *et al.*, J. Phys. Soc. Jpn. **30**, 459 (1971).
[26] M. Born and K. Huang, *Dynamical Theory of Crystal Lattices* (Clarendon, Oxford 1954).
[27] M. P. Tosi, in *Solid State Physics*, edited by F. Seitz and D. Turnbull (Academic, New York, 1964), Vol. 16, p. 1.
[28] *Handbook of Chemistry and Physics*, 54th ed., edited by R. C. West (Chemical Rubber Co., Boca Raton, Fla., 1973—1974).
[29] D. R. Penn, Phys. Rev. **128**, 2093 (1962).
[30] J. M. Ziman, *Principles of the Theory of Solids* (Cambridge, University Press, London, 1964), Sec. 8.2.
[31] M. L. Cohen and T. K. Bergstresser, Phys. Rev. **141**, 789 (1966).
[32] C. Y. Fong and M. L. Cohen, Phys. Rev. **185**, 1168 (1969).
[33] R. L. Zucca, J. P. Walter, Y. R. Shen, and M. L. Cohen, Solid State Commun. **8**, 627 (1970).
[34] J. P. Walter and M. L. Cohen, Phys. Rev. B **1**, 2661 (1970).
[35] L. Ley, R. A. Pollak, S. P. Kowalczyk, F. R. McFeely, and D. A. Shirley, Phys. Rev. B **8**, 641 (1973).
[36] S. Hüfner and G. K. Wertheim, Phys. Rev. B **8**, 4857 (1973).
[37] T. Ishii *et al.*, Phys. Rev. B **12**, 4320 (1975).
[38] A. Kakizaki *et al.*, Phys. Rev. B **28**, 1026 (1983).
[39] J. A. Bearden and A. F. Burr, Rev. Mod. Phys. **39**, 125 (1967).
[40] T. H. DiStefano and W. E. Spicer, Phys. Rev. B **7**, 1554 (1973); R. T. Poole, J. C. Jenkin, J. Liesegang, and R. C. G. Leckey, Phys. Rev. B **11**, 5179 (1975).
[41] C. A. Coulson, L. B. Reder, and D. Stocker, Proc. R. Soc. London **270**, 352 (1962).
[42] J. A. Wilson and A. D. Joffe, Adv. Phys. **18**, 193 (1969).

These authors show, for example, the run of the bond length $d_{M\text{-}X}$ through the nickel halide series: $NiCl_2$, 2.51 Å (experiment) versus 2.35 Å (atomic sum); $NiBr_2$, 2.64 Å versus 2.50 Å, respectively.

[43]P. Pappalardo, J. Chem. Phys. **31**, 1050 (1959); **33**, 613 (1960).

[44]D. J. Robbins and P. Day, J. Phys. C **9**, 867 (1976); E. Wood, A. Muirhead, and P. Day, *ibid.* **11**, 1619 (1978).

[45]J. Van Erk and C. Haas, Phys. Status Solidi B **70**, 517 (1975).

[46]J. Pollini, G. Spinolo, and G. Benedek, Phys. Rev. B **22**, 6369 (1980).